Journal of Controlled Release 358 (2023) 667–680

Contents lists available at ScienceDirect

Journal of Controlled Release

journal homepage: www.elsevier.com/locate/jconrel

Osteoimmunomodulatory GelMA/liposome coatings to promote bone regeneration of orthopedic implants

F. Jahanmard [a,b], A. Khodaei [b], J. Flapper [a,b], O. Dogan [a,b], K. Roohi [c], P. Taheri [c], H. Weinans [b], G. Storm [a], M. Croes [b], E. Mastrobattista [a,*], S. Amin Yavari [b,d]

[a] Department of Pharmaceutics, Utrecht Institute for Pharmaceutical Sciences (UIPS), Utrecht University, Utrecht, the Netherlands
[b] Department of Orthopedics, University Medical Center Utrecht, Utrecht, the Netherlands
[c] Department of Materials Engineering, Delft University of Technology, Delft, the Netherlands
[d] Regenerative Medicine Utrecht, Utrecht University, Utrecht, the Netherlands

ARTICLE INFO

Keywords:
Liposomes
Immune stimulation
Electrospray coating
Hydrogel
Bone regeneration

ABSTRACT

Despite being the most widely used biomaterials in orthopedic surgery, metallic implants do not induce new bone growth because they are bioinert. Surface biofunctionalization of implants with immunomodulatory mediators is a recent approach to promote osteogenic factors that facilitate bone regeneration. Liposomes (Lip) can be used as a low-cost, efficient and simple immunomodulator to stimulate immune cells in favor of bone regeneration. Even though liposomal coating systems have been reported previously, their main disadvantage is their limited ability to preserve liposome integrity after drying. In order to address this issue, we developed a hybrid system in which liposomes could be embedded in a polymeric hydrogel namely gelatin methacryloyl (GelMA). Specifically, we have developed a novel versatile coating strategy using electrospray technology to coat implants with GelMA/Liposome without using adhesive intermediate layer. The two differently charged Lip (i.e., anionic and cationic) were blended with GelMA and coated via electrospray technology on the bone-implant surfaces. The results showed that the developed coating withstood mechanical stress during surgical replacement, and Lip inside GelMA coating stayed intact in different storage conditions for a minimum of 4 weeks. Surprisingly, bare Lip, either cationic or anionic, improved the osteogenesis of human Mesenchymal Stem Cells (MSCs) by inducing pro-inflammatory cytokines, even at a low dosage of Lip released from the GelMA coating. More importantly, we showed that the inflammatory response could be fine-tuned by selecting the Lip concentration, Lip/hydrogel ratio, and coating thickness to determine the timing of the release such that we can accommodate different clinical needs. These promising results pave the way to use these Lip coatings to load different types of therapeutic cargo for bone-implant applications.

1. Introduction

Biological restrictions within the fracture healing process or critical-size bone defects can cause delayed healing or nonunion repair in the skeletal system [1,2]. Despite being the gold standard for bone loss treatment, autologous and allogeneic grafting have not achieved the desired therapeutic impact [3]. Both approaches have several limitations, including insufficient donor supply, limited reproducibility and alteration of material properties due to preparation and sterilization procedures [4,5]. As an alternative approach, bioactive bone-regenerative biomaterials may provide a more optimal and consistent environment for bone healing [6]. Many biomaterials—from metal to polymer—have been used in orthopedic applications, each with pros and cons [7]. Metallic implants are the most widely used biomaterials in orthopedic surgery, owing to their superior mechanical properties [8]. However, they usually fail to induce new bone formation to repair large defects or integrate with the existing bone, due to the bioinert nature and poor bone-mimicking properties of current metallic implants [9]. Implant surface coating with bioactive materials can provide the necessary osteogenic factors for the implant to facilitate the integration with bone [10].

After the bone injury, an initial inflammatory phase is essential to begin the ossification [11,12]. Amongst the different pro-inflammatory mediators, tumor necrosis factor alfa (TNF-a), interleukin-1 (IL-1), and

* Corresponding author at: Utrecht Institute for Pharmaceutical Sciences (UIPS), Utrecht University, Utrecht, the Netherlands.
E-mail address: e.mastrobattista@uu.nl (E. Mastrobattista).

https://doi.org/10.1016/j.jconrel.2023.05.022
Received 27 November 2022; Received in revised form 4 April 2023; Accepted 15 May 2023
Available online 24 May 2023

IL-6 are believed to be the most crucial initial pro-inflammatory cytokines for the fracture healing [13,14]. These cytokines recruit progenitor cells to the injured site, promote their proliferation and differentiation towards osteoblasts, and stimulate the angiogenesis [15,16]. A timely orchestrated inflammatory response is, however, key for optimal bone regeneration, and an excessive, prolonged inflammatory state has an adverse effect on the repair process [17,18]. A recent report showed that the expression of pro-inflammatory mediators, beginning after surgery for 7 days, significantly increased the proliferation rate of MSCs, eventually early stage of healing. Although the excessive or insufficient secretion of these mediators significantly hindered the healing progression [19].

It has been shown that nano- and microparticulate materials are very effective in stimulating immune cells [20]. For instance, the massive internalization of nano/microparticles in macrophages can trigger the NF-kB signaling pathway, resulting in macrophage activation. Liposomes (Lip) have been proposed as suitable nano/microparticles for the delivery of therapeutic agents due to their high biocompatibility and degradability. So far, various liposomal drug formulations have been commercialized and approved in the medical practice [21,22]. To favor immune stimulation, research has mostly focused on using Lip as a carrier to load immunomodulatory agents without sufficient attention to their intrinsic immunomodulatory effects on immune activation [23,24]. Thereby, their inherent effect on immune stimulation and bone regeneration has been left largely unexplored.

To maximize local therapeutic effects and minimize off-target effects, forming a stable film on the implant is beneficial [25]. For regulatory approval, the Lip coating should withstand surgical mechanical stress, and should remain stable at the air-implant interphase under storage conditions prior to surgery. However, in previously reported liposomal coatings through immobilization (e.g., cleavable linkers) has not sufficiently supported the protection of liposomal long-term integrity and activity [26,27]. In the immobilization strategy, the amount of covalently linked Lip to the surface of the implant is also limited by the ultrathin nature of the coating [28], and linked Lip are more susceptible to damage due to dehydration after coating and mechanical forces applied during the surgery [29,30]. Instead, embedding Lip in a polymeric hydrogel [31–33] and applying it on the implant surface with a controlled thickness and crosslink density can act as a suitable temporal controlled release platform for Lip delivery.

Some of the reported coating technologies to apply hydrogels are dip-coating [34], spin-coating [35], spray [36], and electrophoretic coating [37]. However, these coating techniques have some disadvantages in controlling the coating thickness and homogeneity.

Herein, we propose the use of electrospraying [38] that can form a tunable and homogeneous 3D coating with high Lip loading capacity. The advantage of this versatile coating technology is the capacity to precisely control the release of Lip from the hydrogel coating by changing the crosslinking density and thickness of the hydrogel.

In the current work, we aim to lay the foundation for using Lip to stimulate bone regeneration on titanium implants utilizing a mild immune activation. We investigate how factors including liposomal surface charge and lipid content influence their intrinsic immuno-stimulatory and osteogenic effects. It is also hypothesized that forming a stable Lip film on an implant would maximize its local efficacy and minimize undesired systemic effects. To do so, we used gelatin methacrylate (GelMA) as a hydrogel to encapsulate the Lip and used it to apply a homogenous layer on the surface of the implant via the electrospray technique. We investigated the integrity of Lip throughout the entire coating process as well as their intracellular uptake and various storing conditions. To enhance the mechanical interlocking of the coating, electrosprayed GelMA/Lip microparticles were coated onto micro-rough titanium implants. We also assessed the effect of Lip charge and concentration on immune stimulation and osteogenesis. In parallel, the pro-osteogenic effect of released Lip from the coatings was examined.

2. Materials and methods

2.1. Materials

1,2-dipalmitoyl-sn-glycerol-3-phosphocholine (DPPC), 1,2-dioleoyl-3-trimethylammonium-propane (DOTAP), 1,2-dipalmitoyl-sn-glycerol-3-phospho-(1′-rac-glycerol) (sodium salt) (DPPG), L-a-phosphatidyl-ethanolamine-N-(Lissamine Rhodamine B sulfonyl) (Rho-PE) were purchased from Avanti Polar LIPids (Alabaster, AL, USA). Fluorescein isothiocyanate-dextran (60/76kD) (FITC-Dex), Cholesterol (CHOL), Gelatin type A from porcine skin, methacrylic anhydride, HEPES, ethanol, and irgacure were purchased from Merck (St. Louis, MO, USA), and Methanol (BioSolve, Valkenswaard, The Netherlands).

2.2. Lip preparation and characterization

DPPC (25 mg/ml), DOTAP (5 mg/ml), CHOL (20 mg/ml) and Rh-PE (40 μg/ml) were each first separately dissolved in ethanol. DPPG (1 mg/ml) was dissolved in methanol. An anionic formulation is composed of DPPC/DPPG/ Cholesterol at the optimal molar ratio of 63/7/30, and the composition of a cationic formulation is DPPC/DOTAP/ Cholesterol at 61/8/31 M ratio. Both anionic and cationic Lip were prepared using the thin film hydration method. Briefly, A lipid film was prepared by dissolving the lipids and evaporating the organic solvent using a rotary evaporator. The formed dry film was flushed with nitrogen gas to remove all traces of organic solvent. Rhodamine-PE labelled Lip consisted of 0.1 mol% of Rh-PE with respect to total lipid content. 10 mg/mL of FITC-Dex was added to the hydration buffer for FITC labelled Lip. After hydration, the Lip suspension was extruded 10 times through an extruder using an Avanti Mini extruder through 2 × 400 nm polycarbonate filters at room temperature. Finally, the Lip formed after three rounds of ultracentrifugation (Type 70.1 Ti rotor) at 55.000 RPM for 50 min at 4 °C by replacing its supernatant with a volume of HBS that resulted in a theoretical lipid concentration of 30 mM.

The hydrodynamic diameter and the polydispersity index of the particles were measured by dynamic light scattering (DLS; Nano-S, Malvern, UK) after diluting in 10 mM HEPES buffer at pH 7.4. The zeta-potential of the particles was measured at room temperature using a laser doppler electrophoresis (Zetasizer Nano-Z, Malvern, UK). Lipid recovery was measured according to Rouser [39], whereby sodium biphosphate was used as a standard, and the total Lipid content was extrapolated from the concentration of phospholipids.

2.3. Implant

Sandblasted Ti implants (diameter 4 mm; length 25 mm) supplied by Adler Ortho® were used to test the durability of the coating ex vivo using cadaver rabbit tibiae. For the in vitro test setting, solid titanium (Ti) implants (diameter 8 mm; thickness 3 mm), were printed by selective laser melting (SLM) using spherically shaped titanium powder.

2.4. Electrospray coating

GelMA was synthesized as described before [40]. In short, 10% (*w/v*) porcine gelatin type A was dissolved in phosphate-buffered saline (PBS) at 50 °C under constant stirring. Methacrylic anhydride (60% (w/v), MAAH) was added to the prepared gelatin solution. The mixed solution was diluted with 3xPBS to stop the reaction, and the pH was adjusted to 7.4 using 5 mM sodium hydroxide (NaOH). After centrifugation at 4000 rpm to remove excess MAAH, GelMA was dialyzed against deionized water (Milli-Q) at 4 °C for 5 days. Finally, the solution was sterilized by filtering through 0.2 μm pore size and then lyophilized.

The GelMA/water solutions were mixed with liposomal solutions to obtain a blend with a final GelMA concentration of 3 and 6% and various Lip contents (3 mM (Lip(L)) and 15 mM (Lip)). The GelMA/Lip blends were gently mixed at room temperature, followed by the addition of

0.5% irgacure. The prepared solution was injected into a syringe and electrosprayed at the rate of 0.5 ml/h for 15 min. The microparticles were formed after applying the electric field (16 kV), using a high voltage power supply (Heinzinger LNC 30000, Germany). The needle tip distance from the implant was fixed at 10 cm. This resulted in a homogeneous coating being formed on the surface of the implants. After coating, the samples were exposed to UV-irradiation (Bluepoint4 ecocure, Germany) for 2 min to form a stable hydrogel coating. To control the thickness of the coating, the final coating weight was fixed at 3 mg/implant.

2.5. Coating characterization

To verify the intactness of the Lip after electrospraying, the co-localization of the fluorescence signals produced by encapsulating hydrophilic dye (FITC-Dex) in the aqueous core and a Lipophilic dye (Rh-PE) in the shell was studied. The electrosprayed microgels were deposited onto glass slides and imaged by confocal microscopy (Leica SP8X, Germany).

To analyse the distribution and intactness of Lip in the coating, solutions were electrosprayed onto Formvar-coated grids and visualized by transmission electron microscopy (TEM) (FEI Tecnai 12, Thermosystems).

The coating thicknesses were measured by confocal microscopy. The transparent hydrogel containing fluorescent dyes can be detected with this method [41]. The GelMA containing FITC and Rh-PE labelled Lip were electrosprayed on the implant surfaces. The thickness of coated hydrogel was detected using 3d images captured by confocal microscopy.

Attenuated total reflection-Fourier transform infrared spectroscopy (ATR-FTIR, Perkin Elmer Instruments, US) was used to assess the chemical structures of coating surfaces. The transmittance spectra of coated groups were recorded in the range of 600–4000 cm^{-1}. For FTIR measurement, the coated samples were mounted on a sample stage and contacted with an ATR crystal.

The water contact angle of coated samples was calculated by SCA software (SCA20 module, Dataphysics, Germany). The average water contact angle was reported for five measurements performed on each sample.

The AFM measurements were performed on dried coated and non-coated samples using a Bruker-Dimension Edge instrument (BRUKER AXS SAS, France) operating in tapping mode. The microscope was fitted with a Bruker model TESPA probe with an Sb-doped Si cantilever with ~300 kHz resonance frequency. Deflection and height mode images were acquired simultaneously at a fixed scan rate with a resolution of 512 × 512 pixels.

2.6. Degradation and Lip release profile of GelMA/Lip coating

To assess the rate of coating degradation, coated samples were incubated at 37 °C in PBS for 14 days. Media containing degraded GelMA were collected at days 1, 2, 3, 5, 7, and 14. The concentration of degraded GelMA in PBS was estimated using the BCA protein assay kit (Thermofisher, US) according to the manufacturer's instructions. To determine the degradation rate, the concentration of degraded GelMA was normalized to total GelMA content. The total GelMA and Lip contents were measured after complete degradation of the coating.

To determine the Lip release profile, the amount of released Rh-PE labelled Lip (Rh-Lip) was quantified by measuring the Rh signal using a fluorescent reader (Fluoroskan Ascent FL multiplate reader, US) and using a titration of Rh-Lip as a standard. To determine the cumulative release curves, the drug in the release media was normalized to the total drug content.

2.7. Physical stability of GelMA/Lip coating

The physical stability of Lip in GelMA coating was examined after storing them at different temperature-related storage conditions (i.e., room temperature, 4 °C, −20 °C) and after lyophilization. Rh-PE/FITC-Dex labelled Lip were electrosprayed with and without GelMA, named as "GelMA/Lip" and "Lip", respectively. They were sprayed onto glass slides to detect the co-localized signal after 4 weeks of storage in various conditions by confocal microscopy (Leica SP8X, Germany).

For the quantification method, the GelMA containing Lip fluorescently labelled with Rhodamine-PE (Lipid membrane) and FITC-dextran (aqueous interior) Lip were sprayed on the surface of implants. Coated implants were stored at room temperature, 4 °C and 20 °C for 4 weeks. Afterwards, the stored and lyophilized samples were incubated in PBS at 37 °C for 3 days, during which the release of Lip was quantified according to the method described in Section 2.6.

2.8. Durability of GelMA/Lip coating against implantation forces

The ability of the coatings to withstand surgical implantation was tested by implantation into cadaveric rabbit tibiae, as described before [42]. Six sandblasted Ti implants (clinically-relevant implants) were coated with FITC-loaded GelMA. The coatings were visualized before implantation and after explantation by stereo microscopy (Olympus SZX16).

To quantify the remaining coating after removal from the rabbit bone, the explanted implants were washed with demineralized water to remove all the attached tissue residue, subjected to complete drying, and weighted. The removed coating was reported as a weight loss (eq. 1). Where w_0 is coating weight before inserting to the bone and w_1 is coating weight after removing and washing. The washed coated samples were used as a control.

$$weight\ loss\ (\%) = \frac{w_0 - w_1}{w_0} \quad (1)$$

2.9. Cell seeding

RAW 264.7 macrophages (ATCC) and RAW blue cells were cultured in an expansion medium containing Dulbecco's Modified Eagle Medium (DMEM, Invitrogen, US) supplemented with 10% (*v*/v) fetal bovine serum (FBS, Biowest, France), and 1% (v/v) penicillin/streptomycin (Pen-Strep, Invitrogen, US),

Human material was obtained in accordance with the Declaration of Helsinki, with the approval of the local medical ethical committee (University Medical Center Utrecht (UMCU), Utrecht, The Netherlands) under the protocols METC 08–001/K and METC 07–125/C, and with the written consent of the participants.

Human mesenchymal stem cells (MSCs) were isolated and cryopreserved as described previously [43] and were used below passage 4 for all experiments. MSC expansion medium consisted of α-MEM (Invitrogen, US) with 10% (*v*/v) FBS, 1% (v/v) Pen-Strep, and 0.2 mM L-ascorbic-acid- 2-phosphate (Merck, Germany).

Monocytes were isolated from human-blood-derived buffy coats of healthy donors with informed consent. Peripheral blood mononuclear cells were collected by density gradient centrifugation using Ficoll (Merck, Germany), followed by monocyte separation using positive CD14 magnetic-activated cell sorting (MACS), according to the manufacturer's instructions (Miltenyi Biotec, Germany). Monocytes were cultured in a macrophage culture medium consisting of RPMI (Thermo Fisher Scientific, US) supplemented with 10% (*v*/v) FBS and1% (v/v) Pen-Strep in the presence of 25 ng/ml Monocyte Colony-Stimulation Factor (M-CSF, Peprotech, Germany) for 7 days. All cell culture experiments were performed at 37 °C in a humidified atmosphere containing 5% CO_2.

2.10. In vitro experimental groups

The effect of concentration and charge of Lip was investigated using serial dilutions of anionic and cationic Lip (3, 1.5, 0.3, and 0.15 mM) in vitro assays.

To study the effect of released Lip from the coating on cell behavior, the implants coated with 15 mM Lip and 60 mg/ml GelMA were incubated in a cell medium for 24 h, and released Lip were collected for further cell assays.

2.11. Cytotoxicity

To analyse the cytotoxicity, RAW 264.7 cells were seeded at 50,000 cells/well in a 96-well plate in an expansion medium and incubated overnight. The cytotoxicity of all reagents was evaluated with the Alamar blue metabolic activity assay at day 3 by incubating RAW 264.7 macrophages with 10% of AlamarBlue Cell Viability Reagent (Thermo Scientific, US) in an expansion medium. The fluorescence at 544/590 nm was detected using a Fluoroskan Ascent FL multiplate reader (Thermo Labsystems, Finland) after 3 h.

The cell viability was evaluated with a Live-Dead cell staining kit (Thermo Scientific, US) for all experimental groups after 3 days following the manufacturer procedure. The cells were imaged using a confocal microscope (Leica SP8X, Germany). The fluorescence signal from live (green) (500–525 nm) and dead (red) (528–640 nm) cells were processed using Leica software.

2.12. RAW macrophage uptake of lip

The cellular uptake of released Lip/Rh-PE from electrosprayed coating was studied by lysotracker probe (lysotracker red DND-99, Waltham, US). The RAW 264.7 macrophages (50,000 cells/well) were seeded in a 96-well plate. After overnight incubation, the culture medium was replaced with collected released media from coating and 0.5 mM Lip as a reference, followed by incubating at 37 °C for 2 h. Then the medium was replaced with 10 μM of lysotracker red and incubated again for 30 min at 37 °C. Afterward, the cells were washed once with the medium, and the uptake of Lip was detected by confocal microscopy.

2.13. Immune-stimulation of primary and cell line macrophages

Cytokine production by primary macrophages (from human blood monocytes) and cell line macrophages (RAW 264.7) was measured to quantify the immune-modulatory properties of all experimental groups.

Monocytes were seeded at a density of 150,000 cells/well and RAW Macrophage at a density of 50,000 cells/well in 96-well plates. The monocytes were differentiated into macrophages for 7 days in the presence of 25 ng/ml M-CSF. Both primary and cell line macrophages were stimulated for 24 h by the addition of all experimental groups, using Lipopolysaccharide (LPS, from *Escherichia coli* O111:B4, Merck, Germany) at 100 ng/ml as a positive control. The cytokine concentrations in the supernatant were determined by ELISA assay (DuoSet®, R&D Systems).

2.14. Osteogenic differentiation of MSCs

The effect on human mesenchymal stem cells (MSCs) differentiation to brief exposure of Lip (Direct) and macrophage condition media treated with Lip (Indirect) was investigated since the short stimulation of MSCs with mediators can mimic the real in vivo condition [44]. To test the alkaline phosphatase activity (ALP activity) as a marker for bone regeneration, MSCs were seeded at a density of *50*,000 cells/cm^2 in 96-well plate in triplicates. Cells were only treated with mediators during the initial 2 days, while they were continuously exposed to an osteogenic medium (expansion medium supplemented with 10 mM β-glycerophosphate and 10 nM dexamethasone). Osteogenic medium (ODM) lacking Lip served as a negative control and 100 ng/ml LPS as a positive control. The ALP activity was measured after 10 days. Briefly, cells were lysed in 0.2% Triton X-100/PBS for 30 min. ALP activity was measured by the conversion of the *p*-nitrophenyl phosphate liquid substrate system (Merck Fast *p*-nitrophenyl phosphate tablets, Merck, Germany). The absorbance was measured at 405 nm and corrected at 655 nm (Bio-Rad, Hercules). The cell lysate was also used to determine the DNA content with the Quant-It PicoGreen kit (Invitrogen, US), according to the manufacturer's instructions. The ALP/DNA was normalized with cells only treated with ODM.

To assess matrix mineralization, 100,000 MSCs were seeded in 24 well plates in triplicate. Upon 100% confluency, the cells were treated with the same mediators used in the ALP test. For qualitative assessment of matrix mineralization, cells were fixed in 4% (*w/v*) paraformaldehyde for 15 min and stained with 2% (w/v) Alizarin red S solution (pH 4.2, Merck-Aldrich) for 10 min. The mineralized layers were visualized by red staining under light microscopy.

To quantify the amount of deposited calcium, after fixation with 4% (w/v) paraformaldehyde, cells were incubated with 0.2% (w/v) Alizarin Red S for 60 min. Afterward, 10% cetylpyridinium was added for 60 min to extract the calcium-bound Alizarin. Absorbance was detected at 595 nm and corrected at 655 nm.

2.15. NF-κB activation

To analyse the Nuclear factor-κB (NF-κB) activation of RAW-Blue, they were seeded at a density of 10,000 cells/well in a 96-well plate in expansion media (DMEM containing 10% FBS and 1% Pen Strep). The RAW-Blue cells were stimulated in all of the Lip groups for 24 h. The group receiving no Lip served as a negative control, while the group with 100 ng/ml LPS served as a positive control. To determine the NF-κB activation, the *p*-nitrophenyl phosphate solution (pH = 9.6) (Merck, Germany) was added to the collected cell supernatant from each well and incubated for 30 min. The absorbance was measured at 405 nm and corrected at 655 nm (Bio-Rad, Hercules, CA).

2.16. Statistical analysis

Data are presented as mean ± standard deviation. Statistical analyses were performed using SPSS (version 26, IBM SPSS statistic). The Shapiro-Wilk test was used to test normality of the data distribution. The one-way ANOVA with Tukey's posthoc test was used for parametric data. A *P* value of 0.05 was used as a threshold for statistical significance. $*p < 0.05$; $**p < 0.01$; $***p < 0.001$.

3. Results

3.1. Lip characterization

Plain Lip, both anionic and cationic and with an average particle size between 250 and 400 nm were prepared using the Lipid film hydration and extrusion method and dispersed in HBS buffer, pH 7. Anionic Lip exhibited a highly negative zeta potential (−40 mV), due to the presence of PG. Cationic Lip showed a positive surface potential (15 mV), due to the presence of DOTAP. Lipid recovery was reported between 70 and 90% for both anionic and cationic Lip (Table 1).

3.2. GelMA/Lip Coating characterization

All characterizations were performed on electrosprayed GelMA/anionic Lip coating- GelMA/Lip. The schematic illustration shows the process of electrosprayed Coating of GelMA/Lip on the implant surface (Fig. 1a).

The SEM images showed the surface morphology of implants before and after coating with GelMA and GelMA/Lip (Fig. 1b). The presence of Lip in the GelMA coating was confirmed by AFM which reflected more

Table 1
Characteristics of prepared anionic and cationic Lip.

Type of Lip	Molar ratio of Lipids	Hydrodynamic diameter (nm)	Poly dispersity index	Zeta potential (mV)	Lipid recovery (%)
Anionic	DPPC/DPPG/Cholesterol (63/7/30)	270	0.097	−40	85
Cationic	DPPC/DOTAP/Cholesterol (61/8/31)	400	0.169	+15	78

roughness on the implant surfaces (Fig. 1c); these images were presented in 2D and 3D. The contact angle measurements indicated that the surface wettability of the implant increased by applying either GelMA or GelMA/Lip on the surface, while the incorporation of Lip in the coating didn't change the surface free energy of GelMA (Fig. 1d). This finding suggests full encapsulation of Lip in GelMA.

The GelMA infrared spectrums showed peaks at 1526, 1645, and 3284 cm^{-1} related to N—H bending (amide II), the C═O stretching (amide I) and N—H stretching (amide A), respectively. No extra peaks were observed for GelMA/Lip groups, which confirmed our finding regarding the encapsulation of Lip by the contact angle method (Fig. 1e). The coating thicknesses were assessed by confocal microscopy equipped with laser-induced fluorescence (LIF) system, which uses the laser beam to penetrate the coated hydrogel. The confocal images showed a thickness of the coating in the range of 30–60 μm, depending on the electrospraying time (Fig. 1f).

The Lip distributions in GelMA electrospray droplets were visualized by fluorescence confocal microscopy. The red signal of Lip labelled with Rhodamine showed how Lip were distributed in electrospray droplets. The image showed a relatively uniform distribution of Lip inside the droplets (Fig. 1g).

3.3. Integrity of Lip in hydrogel coating

To demonstrate the integrity of Lip embedded in GelMA we applied both transmission electron microscopy (TEM) and confocal laser scanning fluorescence microscopy (Fig. 2).

The schematic illustration (Fig. 2a) shows the studied area of GelMA/Lip microgels characterized by TEM and confocal microscopy. TEM images showed the presence of intact Lip(L) (3 mM) and Lip (15 mM) in GelMA droplets (Fig. 2b). Intact Lipid bilayers can be discerned. Moreover, density differences between the GelMa background and the interior of liposomes demonstrate the intactness of individual liposomes. This was further confirmed by LCSM (Fig. 2c), in which fluorescent FITC-dextran was entrapped inside the aqueous core of liposomes and rhodamine in the liposomal bilayer. Damage of liposomes would lead to leakage of FITC-dextran from the liposomes and dilution over the GelMA droplet. Fluorescence images show co-localization of FITC and Rh signals indicative of intactness of Lip in GelMA droplets for both Lip and Lip (L) groups. It was also observed that increasing Lip concentrations led to more agglomeration in the hydrogel (Fig. 2c). For the further experiments, 6% GelMA was selected due to its ideal ability for electrospraying.

We further tested the uptake of double-labelled Lip, either released from the GelMA microgels or added to the cell culture medium into RAW 264.7 macrophages. Confocal microscopy showed co-localization of FITC-Dex and Rh inside endocytic compartments in RAW 264.7 macrophages for released Lip and Lip(L) groups, while Lip(L) and Lip blended with GelMA as a control (Fig. 2d). Together, these results showed that the Lip preserved their integrity throughout the coating process and cell internalization.

3.4. Physical stability and mechanical durability of GelMA/Lip coating

To show the stability of Lip in GelMA microgel over a period of 4 weeks, Lip carrying the hydrophilic FITC-Dex (green) in their core and Lipophilic Rh-PE (red) in their shell were electrosprayed on glass slides. Water/Lip (i.e., no GelMA) was used as a control. The confocal images displayed the co-localization of red and green signals in GelMA/Lip groups (not water/Lip groups) at room temperature and 4 °C, which demonstrated Lip ability to preserve their integrity during 4 weeks (Fig. 3a). However, freezing GelMA/Lip coating at −20 °C induced shrinkage in the microgel, which is most likely the consequence of nucleation of ice crystals after freezing [45], which can affect the Lip stability in the coating. The effect of lyophilizing was also studied on the stabilization of Lip in which freeze-dried Lip without any lyoprotectant agents led to full degradation of Lip, while the presence of GelMA as serves as lyoprotectant resulting in improved Lip resistance to degradation during lyophilization procedures.

To quantify the Lip stabilizing potential at different storing temperatures over a period of 4 weeks and after lyophilization, the release of Lip from the GelMA coating were studied after 3 days incubation in PBS (Fig. 3b). The results showed no significant difference between released Lip after and before storage, however, a slightly decrease in Lip released was observed between groups stored at −20 °C and undergoing lyophilization (before storage).

The schematic illustration elucidated the GelMA serves as a lyoprotactant agent to protect Lip integrity after rehydration (Fig. 3c). Together, these results indicated encapsulation of Lip within the GelMA matrix as lyoprotectant agent, which prevented particle aggregation and protected them against the mechanical stress of freezing and drying.

To test whether the coating could withstand the mechanical shear forces posed upon it during handling and press-fit implantation, coated Ti rods were applied to a cadaveric rabbit bone (Fig. 3d). Examination of implants showed no signs of coating delamination or deformation. Of note, the bones had to be completely broken to allow retrieval of the implants, showing the firm fixation that was applied. To quantify the GelMA/Lip coating resistance to mechanical forces during implantation, the weight loss of coatings after removing from the cadaveric bone were investigated (Fig. 3e). The results verified that only 15% of the coating weight was lost during this procedure which potentially reflects durability of the developed coating respect to the applied forces during the surgery. This can be explained by the strong bond between implant and electrosprayed microgels. The cumulative effect of many non-covalent bonds (e.g., dipole−dipole interactions and van der Waals forces) between microgels and metal surfaces enhanced the interfacial interaction and collectively leads to high bonding energy. In addition, the roughness of implant improved the mechanical interlock between microgels and metal.

3.5. Release and degradation of GelMA/Lip coating

The elevation of pro-inflammatory cytokines during the first-week post-fracture is noticeable, specifically in the first 24 h [46]. In addition, the influence of pro-inflammatory cytokines on recruiting MSCs becomes significant from day 3 post-fracture [19]. To optimize the GelMA concentration and UV crosslinking time of the coated hydrogel, the degradation rate of GelMA and Lip release were investigated. In particular, 3% and 6% GelMA (3G and 6G) were blended with 15 mM Lip and electrosprayed on the implant surfaces, followed by crosslinking for 2 and 6 min, respectively (Fig. 4a).

Minimum GelMA concentration and short crosslinking time (3G 2 min group) showed faster GelMA degradation and higher initial burst release of Lip from coating. In all groups, >80% of Lip were released after 3 days and almost 100% after 7 days, which are in line with the GelMA degradation profile. However, around 80% of GelMA in all groups degraded over 14 days.

The release profile of GelMA coating supplemented with either 3 mM

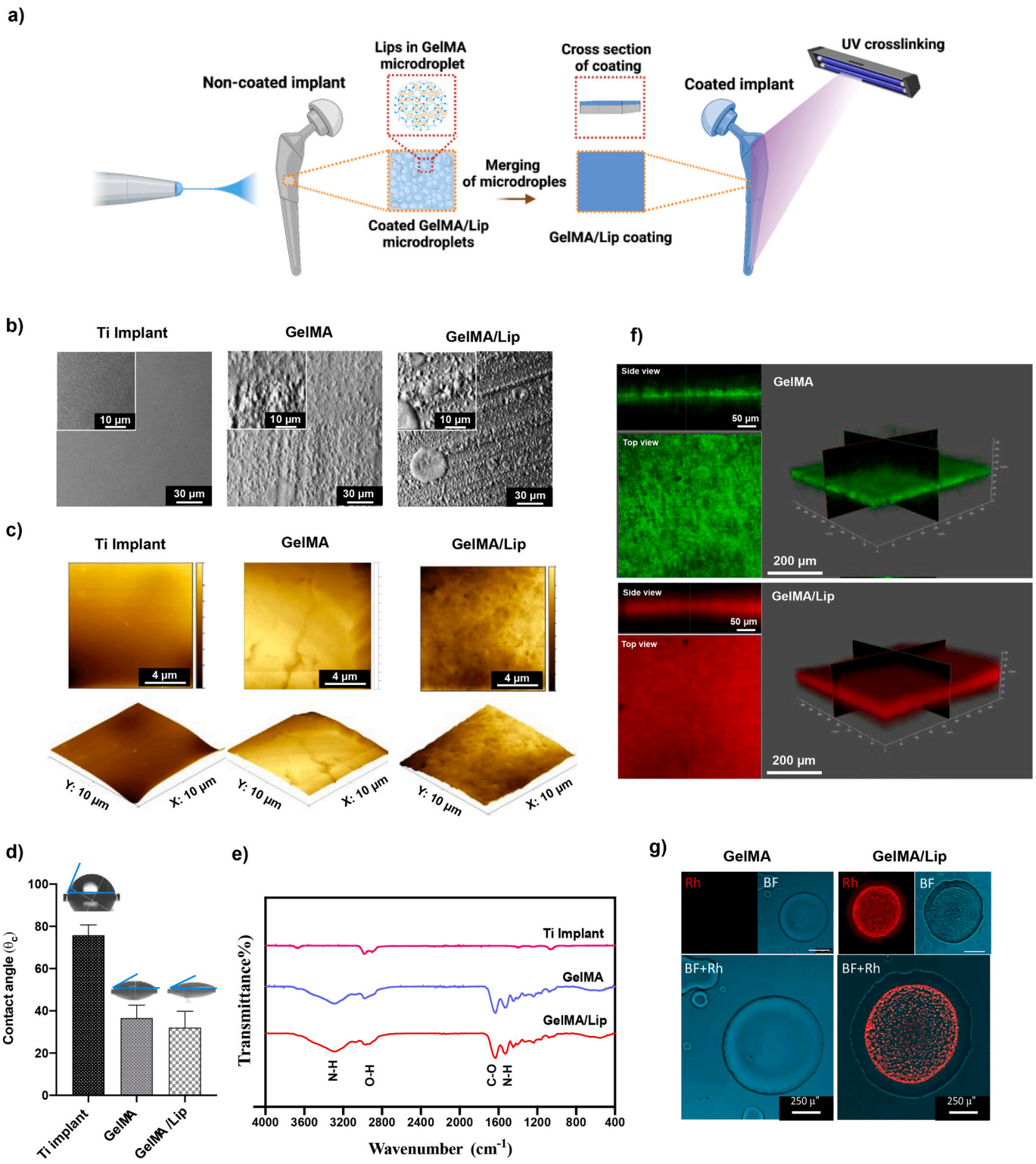

Fig. 1. GelMA/Lip Coating characterization (a) Schematic illustration of GelMA/Lip coating formation (b-c) SEM and AFM images of Ti implants before and after coating with GelMA and GelMA/Lip (d) Water contact angles of the hydrogel coatings ($n = 5$) (e) FTIR spectra of GelMA and GelMA/Lip (f) Coating thickness of hydrogel coatings, determined by confocal microscopy (g) Lip distribution in the microgel-formed coating, visualized by confocal microscopy. Data are represented as the mean ± SD.

(Lip(L)) or 15 mM (Lip) Lip were also tested (Fig. 4b). The cumulative release profiles show more burst release in Lip groups during the first day. For both groups, >80% of Lip were released during the initial 3 days. The degradation profile of GelMA showed the highest degradation rate in the first 2 days which explains the higher released rate of Lip. Release of cationic and anionic Lip (15 mM) from 6% GelMA coating as well as GelMA degradation were also studied. The results showed a higher release of anionic Lip compared to cationic Lip over 14 days, which could be due to the repulsion forces between negatively charged-GelMA and negatively charged Lip, the smaller size of anionic Lip and

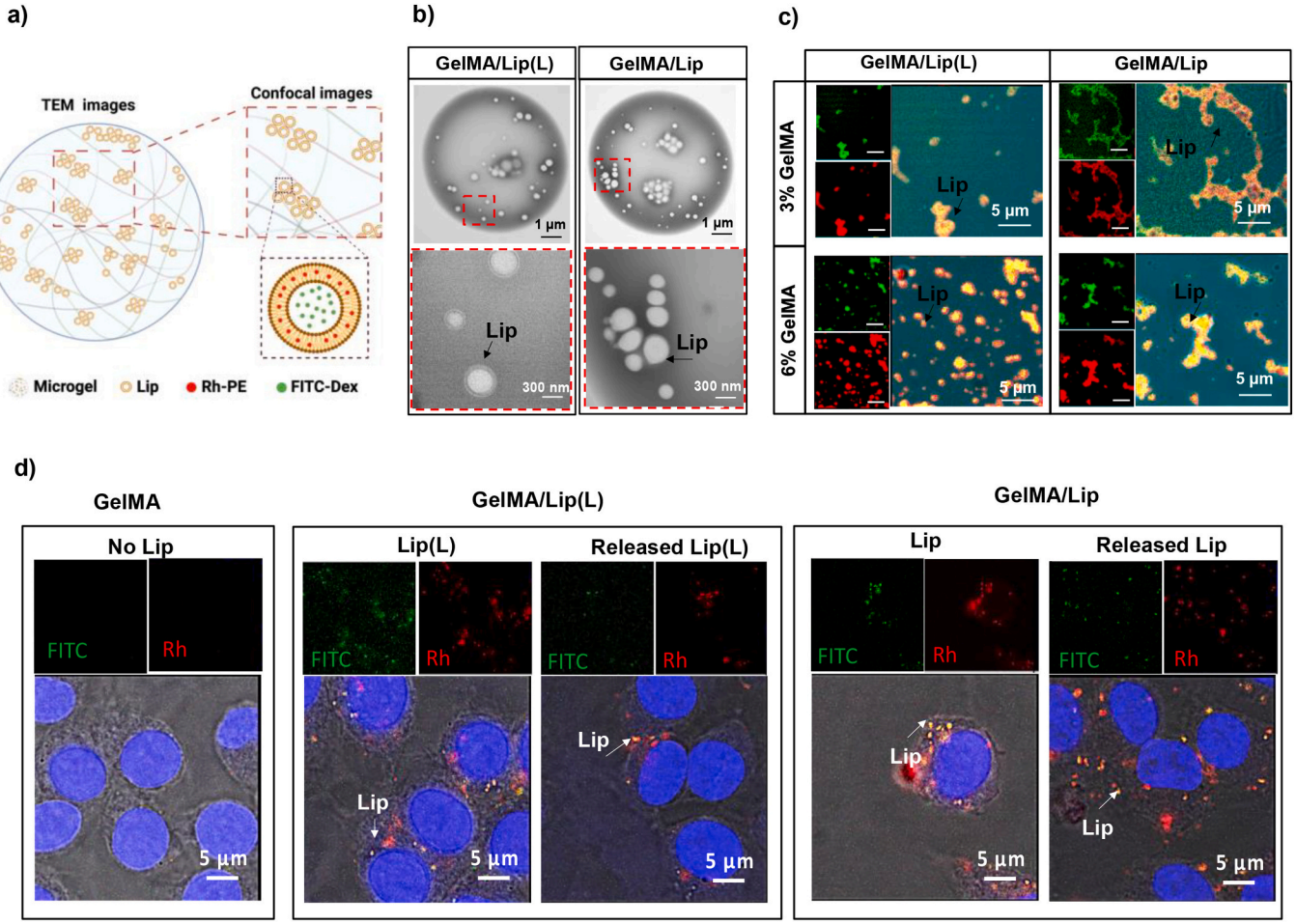

Fig. 2. Verification of the intactness of FITC-Dex/Rh double-labelled Lip after electrospraying (a) Schematic illustration of Lip in microgel-formed coating to depict the areas characterized by TEM and confocal images. The hydrophilic FITC-Dex and Lipophilic Rh-PE were encapsulated in the core and shell of Lip, respectively (b) TEM images of electrosprayed GelMA microgels containing Lip(L) (3 mM) and Lip (15 mM) (c) Confocal images of Lip electrosprayed on glass slides showing co-localization of FITC-Dex (green) and Rh-PE (red) signals. The 3% and 6% GelMA solution was supplemented with 3 mM Lip (Lip(L)) and 15 mM Lip (d) Confocal images showing intracellular uptake of Lip by RAW 246.7 macrophages in both direct addition and released Lip in media during 24 h. Co-localization of FITC-Dex (green) and Rh-PE (red) signals can be seen with clustering around the cell nuclei. Nuclei were stained with DAPI (blue). (For interpretation of the references to colour in this figure legend, the reader is referred to the web version of this article.)

faster degradation of GelMA. Approximately 80% of anionic Lip and 60% of cationic Lip were released during the first 3 days. Altogether, a higher GelMA and Lip concentration, as well as a relatively low GelMA crosslinking time were deemed optimal to favor Lip release to provide the necessary immunomodulation during bone regeneration.

3.6. Cytotoxicity and immune stimulation of Lip

Cytotoxicity of all Lip experimental groups were determined using live-dead, Alamar blue and Picogreen staining. Macrophages were treated overnight with serial dilutions of Lip of both anionic and cationic groups followed by collecting the release media within the first 24 h. An increased number of dead cells were found after treatment with a higher concentration of cationic and anionic Lip, while no dead cells were observed in the released Lip and lower concentration (<1.5 mM) of Lip groups (Fig. 5a).

Moreover, no significant differences were observed in metabolic activity and DNA contents of all Lip experimental groups (Fig. 5b and c), which indicated no cytotoxicity of either anionic or cationic Lip. We also examined the cellular uptake and accumulation of the released Lip in lysosomes by staining live cell lysosomes with a lysotracker probe (Fig. 5d). A strong co-localization of Rh-PE labelled Lip (red) with Lysotracker fluorescent dye (green) was observed, which validates the lysosomal localization of released either cationic or anionic Lip in macrophages (0.5 mM Lip used as a control).

In the early stages of bone fracture, first 7 days, the pro-inflammatory cytokines, including IL1, IL6, and TNFα are an essential signal for the initiation of bone regeneration, followed by expression of anti-inflammatory cytokines, including IL4, IL10, and IL13 in the late stages of inflammation to complete fracture healing [46,47].

To study the effect of Lip groups on the immune stimulation of macrophages, the expression of two pro-inflammatory (IL-6 and TNF-α), an anti-inflammatory (IL-10) and NF-κB activation were investigated. In short, the results showed a dose-dependent expression from all the examined cytokines, except for IL-6 expression of the cationic Lip (Fig. 5e). A higher concentration of anionic Lip groups revealed more expression of IL-6 and IL-10 compared to cationic groups. The released Lip from coating showed a significant difference with control (no Lip) in pro-inflammatory TNF-α expression in both cationic and anionic groups. In this study, we also found that our platform could achieve similar immune stimulation as the gold standard LPS. For NF-κB cytokine expression, all Lip groups could enhance the NF-κB activation in a dose-dependent manner. To illustrate, 3 mM and 1.5 mM of cationic and anionic Lip showed a similar activation of NF-κB as the LPS group. This indicates that the immune response initiated by the Lip is mediated through NF-κB activation. The higher activation of released Lip group

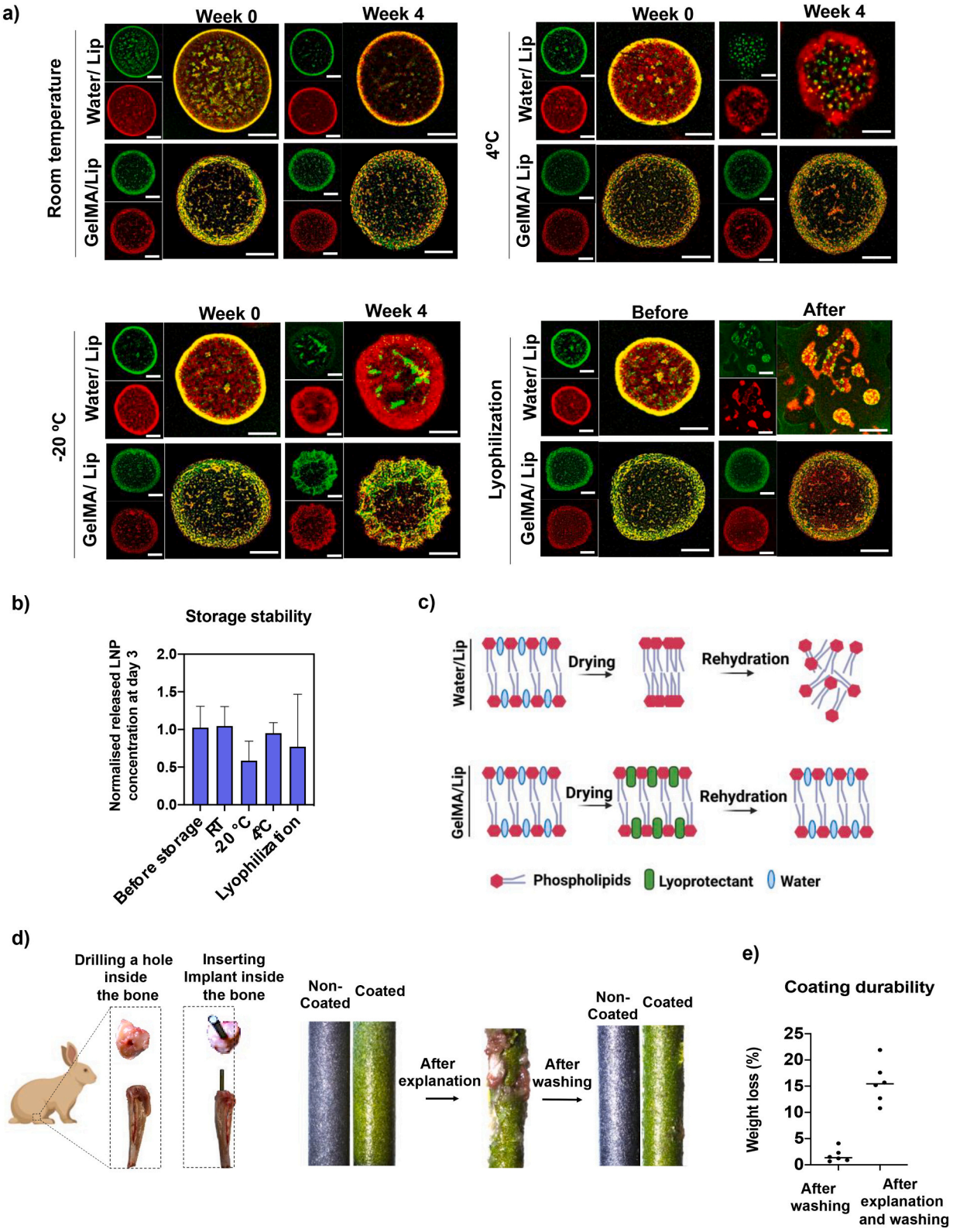

Fig. 3. Physical stability of Lip in GelMA microgel and durability of hydrogel coating against implantation during surgery (a) Confocal images of electrosprayed microgel of GelMA/Lip and water/Lip (no GelMA) before (week 0) and after (week 4) storing in different temperature-related conditions (room temperature, 4 °C and − 20 °C) as well as before and after lyophilizing procedures, scale bar: 60 μm (b) Quantifying the Lip resistance to destabilizing under different storage conditions. Data represent the means ± SD ($n = 3$). Destabilizing by recording the Lip release after 3 days incubation in PBS before and after storage (c) Schematic illustration of GelMA mechanism to protect Lip from destabilization (d) Press-fit implantation of the implant, coated and non-coated with GelMA/Lip labelled with FITC-Dex (green) in a cadaveric rabbit bone to show coating durability (e) Quantification of weight loss of GelMA/Lip coating after explantation from cadaveric bone by weighing the implant before and after explantation. (For interpretation of the references to colour in this figure legend, the reader is referred to the web version of this article.)

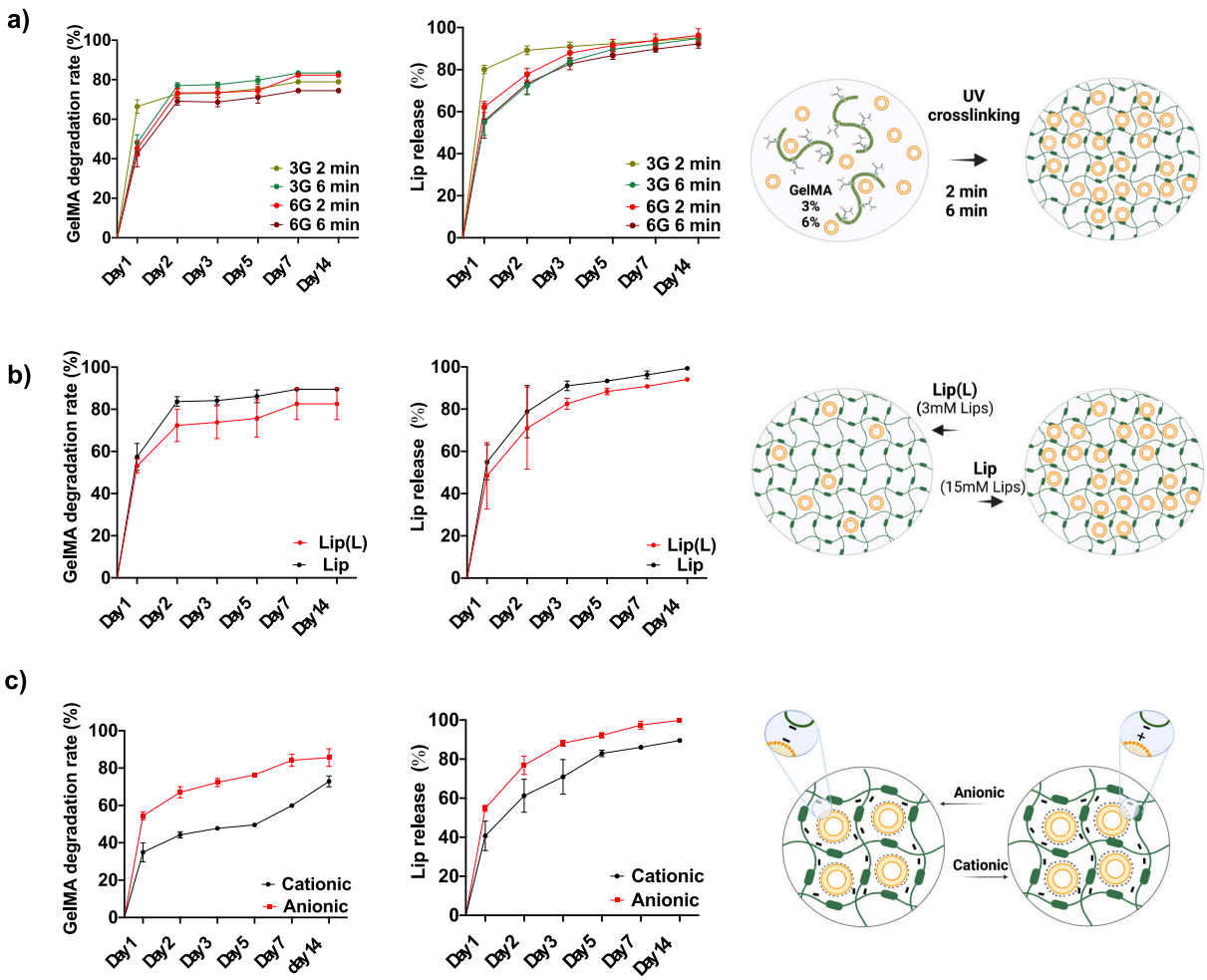

Fig. 4. Hydrogel coating degradation and release profile (a) 3% and 6% GelMA solution were blended with 15 mM Lip, electrosprayed on the implant, and crosslinked by UV for 2 and 6 min (b) GelMA/Lip coating with 3- and 15-mM Lip concentrations (i.e., Lip(L) and Lip) (c) GelMA/Lip (6% GelMA/15 mM Lip) coating with positive and negative surface charge (i.e., cationic and anionic). Data represent the means ± SD ($n = 3$).

could show the synergistic effect of GelMA and Lip in NF-κB activation (Fig. 5f). We have successfully mimicked the initial inflammatory phase needed for optimal bone regeneration. We showed that the inflammatory response can be fine-tuned, by selecting the Lip concentration, Lip/hydrogel ratio and coating thickness to determine timing of release, such that we can accommodate different clinical needs.

3.7. Immune stimulation of human macrophages and osteogenic differentiation of MSCs after short exposure to Lip

Human macrophages were subjected to Lip formulations for 24 h to study their immunomodulatory effect. Similar to RAW macrophages, they expressed both pro and anti-inflammatory cytokines in a dose-dependent manner. High concentrations of Lip (>0.15 mM) resulted in higher expression of all inflammatory cytokines compared to the LPS positive control. Low concentrations of Lip and GelMA released Lip induced only pro-inflammatory cytokines which is actually necessary for the inflammatory stage of bone healing.

To determine the role of Lip in osteoblast differentiation, alkaline phosphatase (ALP) activity and mineralization of MSCs were investigated. It was observed that short treatment with most of the Lip test settings didn't increase the ALP activity (Fig. 6b), whereas 0.03 mM Lip and GelMA-released Lip groups showed a different trend (Fig. 6b). These observations suggest that short exposure of MScs to the low dosage of inflammatory mediators could induce early osteogenesis. The optimal concentration of pro-inflammatory cytokines in fracture healing could enhance the early stage of healing and excessive or insufficient secretion of these signals could hinder the healing progression [19].

Studying the matrix mineralization of different groups verified a significant increase in the calcium deposition by MSCs cells after treatment with the treated conditioned media of macrophages with Lip groups (Fig. 6d). The highest matrix mineralization was seen at released Lip groups for both cationic and anionic groups. These data suggest that low dosage of the Lip groups enhances not only the early osteogenesis but also the late osteogenic differentiation. The short exposure of MSCs to release Lip groups induced the highest osteogenic differentiation, explaining the synergistic effect of degraded GelMA in promoting osteoblast differentiation.

4. Discussion

We developed a tunable GelMA/Lip coating system for orthopedic implants, in which Lip have been embedded in the GelMA coating. This versatile coating platform permits 1) loading of Lip without losing their integrity and 2) tuning the release by modifying the hydrogel and coating parameters, which are essential in designing a local liposomal drug delivery system with enhanced functionality and efficacy.

Lip size, charge, and Lipid composition are important modalities to harness macrophage engulfment and stimulate or suppress the immune response [48,49]. We synthesized the Lip in a range of 200–500 nm, which can be optimally taken up by macrophages [50]. The justification for this size range is that small particle sizes (<1 μm) can be internalized

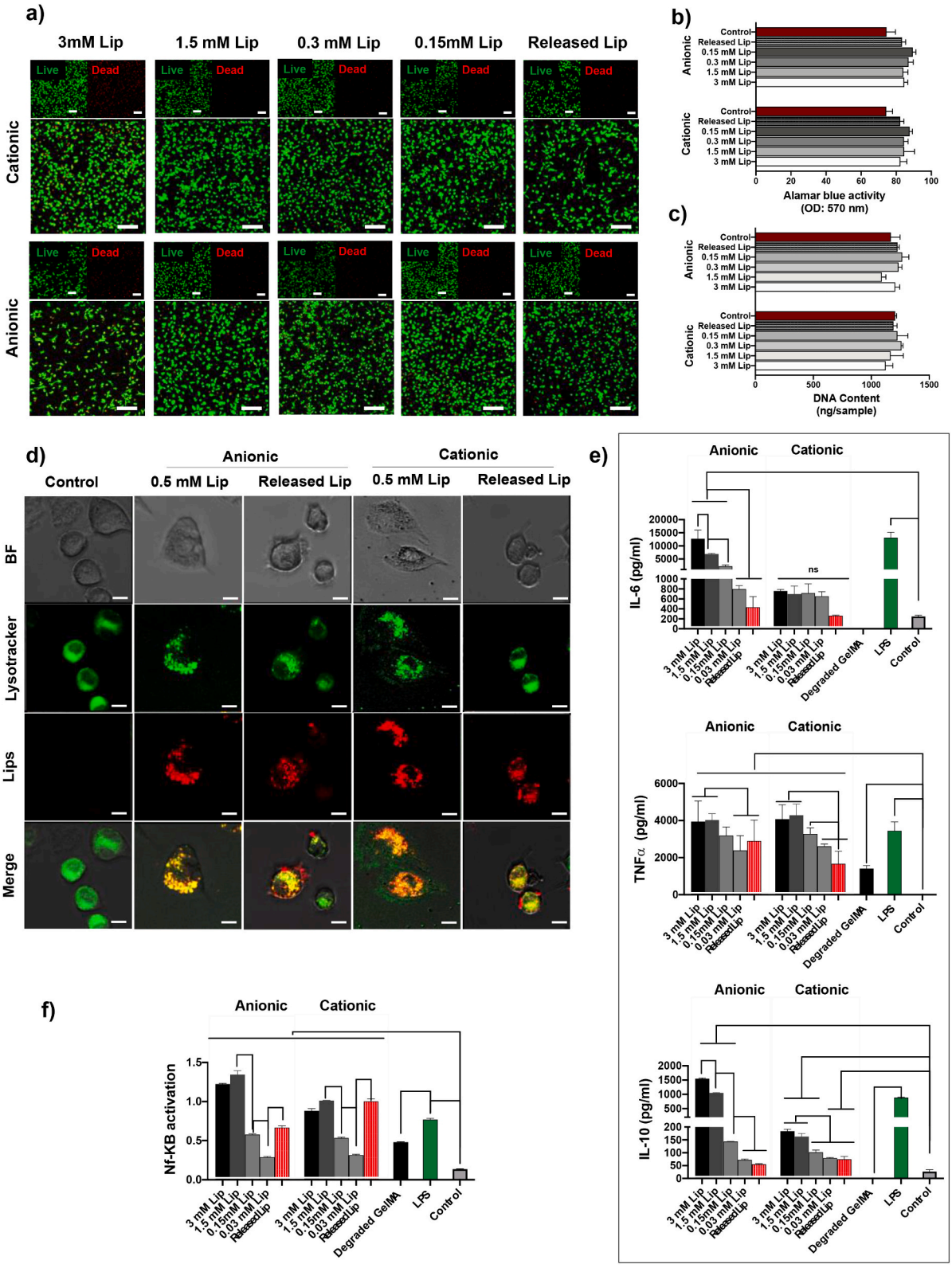

Fig. 5. Cell viability of RAW macrophages after exposing to all Lip experimental groups (a) Confocal images of Live-dead staining of cells (scalebar = 100 μm) (b) Alamar blue quantification of metabolic activity (c) Picogreen DNA assay to quantify DNA contents of cells (d) Confocal images of the cellular uptake of Lip in released Lip from coating and 0.5 mM Lip as a control, Lysosomes and Lip are stained in green, and red, respectively (scalebar = 10 μm) (e) Pro-inflammatory (TNF-α and IL-6) and anti-inflammatory (IL-10) cytokine expression of RAW macrophages stimulated 24 h with Lip (f) Nuclear factor-κB (NF-κB) activation of RAW macrophages after 1 day exposure to all experimental groups; LPS as a positive control, Degraded GelMA as a control for Released Lip group and the groups receiving no Lip (Control) as a negative control. Data represent the means ± SD (n = 3) *P < 0.05 / **P < 0.005/ ***P < 0.001. (For interpretation of the references to colour in this figure legend, the reader is referred to the web version of this article.)

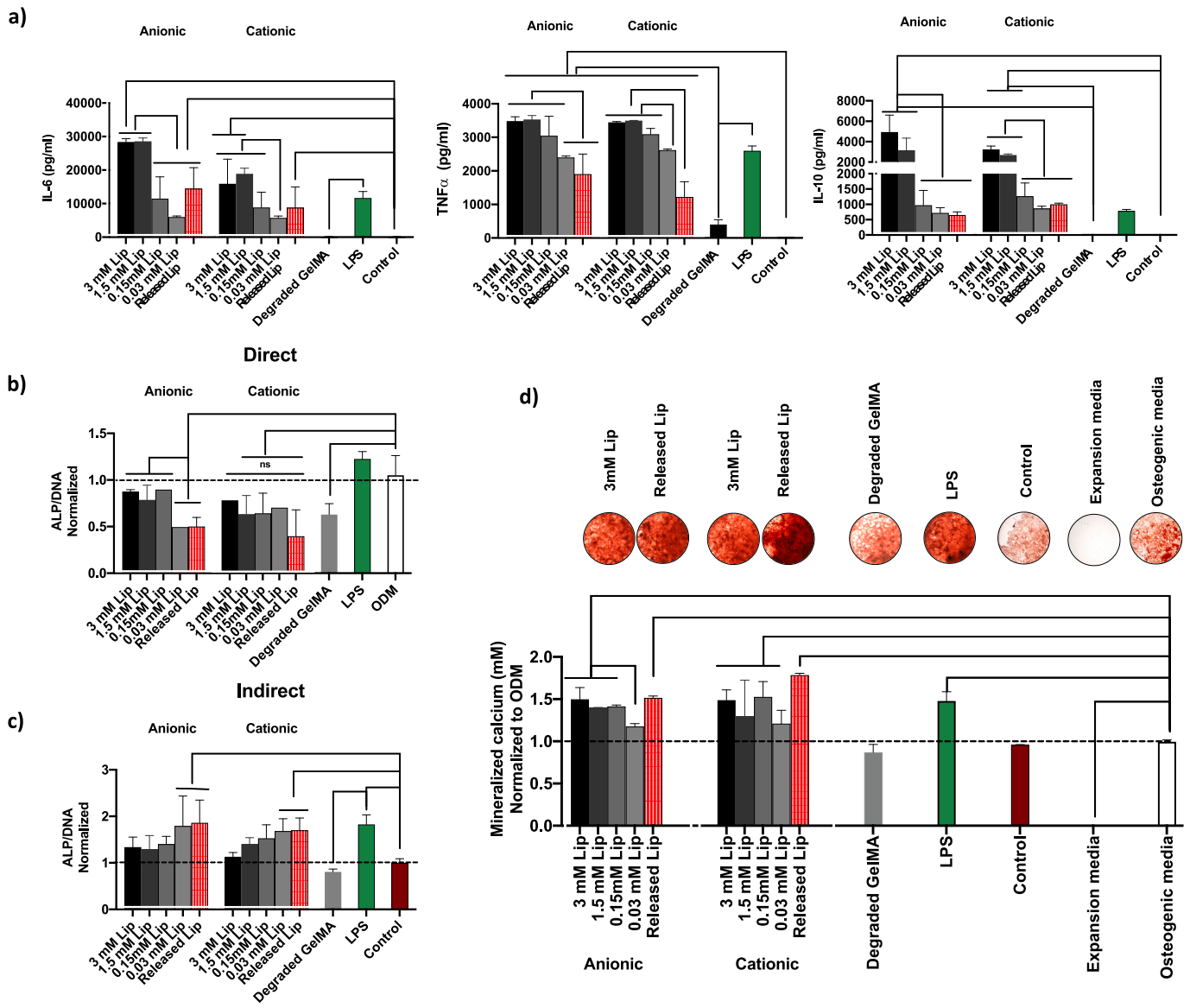

Fig. 6. Immune stimulation of human macrophages and osteogenic differentiation of human mesenchymal stem cells (MSCs) after short exposure to Lip groups (a) Pro-inflammatory (TNF-α and IL-6) and anti-inflammatory (IL-10) cytokine expression of human macrophages stimulated 24 h with Lip groups. (b) Alkaline phosphatase (ALP) activity of MSCs exposed to the Lip groups (Direct method) (c) ALP activity of MSCs exposed to conditioned media of macrophages treated with Lip groups for 24 h (Indirect method), The ALP activity was measured after 10 days and normalized for DNA content. (d) Quantified calcium deposition at day 21; LPS as a positive control, Degraded GelMA as a control for released Lip groups, macrophage conditioned media without Lip (Control) as a negative control; all the data was normalized to the cells exposed to osteogenic media (ODM) only. Data represent the means ± SD ($n = 3$) $^{*}P < 0.05$ / $^{**}P < 0.005$/ $^{***}P < 0.001$.

in the cells and secrete excessive levels of cytokines, resulting in a more desirable level of inflammation [51]. On the other hand, bigger particle sizes (> 3 μm) cannot be readily taken up by macrophages to propagate the inflammatory response [50]. The Lip's surface charge is another crucial factor that affects cell internalization, the endocytosis mechanism, and the immune activation [52,53]. There have been contradicting reports on whether the negative or positive charge is optimal for phagocytosis by macrophages and, thereby their activation. It has been reported that cationic Lip are more potent in cell internalization and immune activation than anionic and neutral Lip due to electrostatic attraction between the cationic particles and negatively charged cell membranes. Moreover, positively charged Lip can induce an antigen-specific cellular immune response [52,54]. However, a similar extent of phagocytosis in cationic and anionic Lip has been reported in phagocytic cells such as macrophages [55]. Some studies have shown that anionic Lip induced an immune response through secretion of interleukin 12 (IL-12) and interferon (IFN- γ) [56].

In the current study, we showed that Lip with the positive or negative surface charge led to a similar macrophage activation (Fig. 5), which favors the same level of osteogenesis (Fig. 6).

Compared to other nanoparticles, especially polymeric particles, a major drawback of liposomal coating systems is their limited potential to stay intact after coating [27,57]. We addressed this issue by developing a hybrid system wherein Lip is embedded in a polymeric hydrogel. Natural hydrogels such as collagen, hyaluronic acid, chitosan, and gelatin have been used extensively in biomedical applications due to their high biocompatibility and degradability and being an environmentally friendly material [58]. We selected gelatin hydrogel as a lyoprotectant support [59] for Lip and proved that this provided for their physical stability in a wide range of environmental or storage conditions (e.g., different storage temperatures) (Fig. 3a). Gelatin hydrogel helps Lip reconstitute their counterparts into their original structure upon hydration [60]. Crosslinking, either physically [61] or chemically [62], is another essential requirement to form a 3D network needed for

hydrogel stability. Photoinitiated crosslinking [63] is a promising method to solidify hydrogel without damaging the Lip structure. We chemically modified gelatin with methacrylic anhydride to create a photo cross-linkable natural hydrogel named GelMA [64]. We found that GelMA can support Lip against fusion, aggregation, and collapse during the coating procedures, storing, and bone implantation in clinical application due to the lyoprotectant effect.

The key challenge in hydrogel coating is overcoming the weak interaction between the hydrogel and the substrate, which normally leads to delamination and detachment of the hydrogel coating upon contacting the water [65]. A standard method to improve the interfacial strength between hydrogel and metal is modifying the metal surfaces with either an adhesive intermediate layer like cyanoacrylate [66] or a linker like carboxylic acid, silanes, polydopamine, and phosphonates that can bridge the interface between the hydrogel and metal [34]. A thin hydrogel coating, however, requires an adhesive-free interface due to the diffusion of the adhesive into the hydrogel [34]. Linker molecules can also change the chemical structure of hydrogel with multiple processes in relatively harsh conditions [67], which might affect the intactness and distribution of Lip in the hydrogel. To circumvent these challenges, we used an electrospray coating technology to coat the implant using spray-charged microdroplets through applied electrostatic force to hydrogel fluid, followed by merging the microgels and forming a uniform coating [68,69]. In this approach, strong physical and non-covalent bonding is formed between the electrospray microgels and rough implants- with a more exposed interfacial area- which reduces the probability of coating delamination during implantation in the bone [70].

Besides fine-tuning the physical properties of GelMA/Lip coating, tailoring the Lip release profile to stimulate immune cells, specifically macrophages [71], is necessary for the early inflammatory phase of fracture healing. The expression of pro-inflammatory cytokines such as TNF-α and IL-6 in the initial inflammatory stage is crucial to recruit monocytes and skeletogenic mesenchymal stem cells and form a pro-regenerative environment. For example, recent reports showed that a low dose of pro-inflammatory cytokines such as TNF-α during the first 7 days post-fracture is essential for recruiting MSCs and subsequently stimulate fracture healing [19]. However, a transient inflammatory response appears optimal, since a prolonged or dysregulated expression of or-inflammatory cytokines typically has a detrimental effect on osteogenesis and bone healing [17,46]. Thus, we hypothesized that a timely and controlled release of Lip in the early inflammatory window of fracture healing, inducing sustained expression of pro-inflammatory signals, is a promising strategy to generate a pro-osteogenic environment. The desired Lip release kinetic from GelMA hydrogels was achieved by fine-tuning the coating parameters such as crosslinking density, GelMA/Lip concentrations, and hydrogel thickness. Our optimized Lip-loaded coating system resulted in an initial burst release of both cationic and anionic Lip, followed by fast release over 3 days and slow release from day 3 to 7 (Fig. 4c).

We further investigated the role of Lip charge and concentration on cytokine expression of either a mouse macrophage cell line (RAW 264.7 cells) or human macrophages following release from the coating. We found a dose-dependent effect of both cationic and anionic Lip on stimulating TNF- α, IL-6 (i.e., pro-inflammatory cytokines) and IL-10 (i.e., anti- cytokine) in both human and mouse macrophages, albeit these effects were more prominent for the anionic Lip. It appears that the established cytokine profile by the current Lip coating may induce a robust osteogenic response in vivo. TNF- α acts as a chemotactic agent to recruit necessary cells to the site of injury and is responsible for recruiting and regulating the osteogenic differentiation of MSCs. IL-6 can stimulate angiogenesis, produce vascular endothelial growth factor (VEGF), and regulate osteoblasts and osteoclast differentiation [14,46]. IL-10 plays a crucial role in the resolution of inflammation and initiating subsequent bone healing [17,72]. Of note, quantifying the level of these cytokines can also be considered the initial step to distinguishing between macrophage phenotypes. Further investigations are, however, needed to elucidate the process of monocyte differentiation in forthcoming research.

ALP activity (an early osteoblast marker) and bone mineralization (a late osteoblast marker) are routinely used in in vitro osteogenesis assays to test the differentiation of osteoblast precursors such as MSCs [73]. We have previously shown that pro-inflammatory signals such as TNF- α can enhance the ALP activity of MSCs together with an osteogenic stimulus [74]. Here, we showed that the cocktail of cytokines cocktails produced by macrophages after Lip phagocytosis elevated the ALP activity of MSCs, while the direct addition of Lip groups to the MSCs did not achieve this effect. The pronounced effect on ALP activation was seen in groups with the lowest Lip concentration and released Lip from the coating, demonstrated by the fact that low dosages of pro-inflammatory and no anti-inflammatory cytokines can augment the fracture repair [75]. However, our ALP results did not completely predict the in vitro matrix mineralization results. We found that all Lip groups significantly enhanced the matrix mineralization, specifically Released Lip from the coating. It can be explained that mineralization is mainly induced by IL-6 and not TNF- α, and our mineralization results have followed the trend of the IL-6 expression [76]. Furthermore, the combination of Lip and GelMA induced a synergistic response in the matrix mineralization. Possibly, induced via endogenous endotoxins in GelMA [77].

The current GelMA/Lip coating can be considered a versatile delivery system platform for delivering Lip with or without various cargos in different clinical applications. Loading multiple cargoes using this coating is of interest since the temporal release of each cargo can significantly improve the functionality of the coating. For example, to enhance the bone regenerative effect of this system, we propose to load chemokines directly in GelMA and pro-inflammatory mediators such as PAMPs or LPS in the Lip to regulate the temporal release. Faster release of chemokines can recruit more immune cells to the injury site, and subsequently, the release of subsequent inflammatory mediators can enhance the osteogenesis process.

5. Conclusion

A versatile liposomal coating technology for bone implants that could stimulate osteogenesis was developed using electrospraying. The GelMA/Lip thin film layer was coated on the implant surfaces without compromising the Lip integrity and activity. A firmly anchored bioactive Lip coating withstood the mechanical shear forces during surgical replacement. Interestingly, it was shown for the first time that the developed stable GelMA/Lip coating could be stored at room temperature for a long time (i.e., 4 weeks). Moreover, most freeze-dried Lip in coating remained intact after complete drying. These physical properties of the developed coating, such as stability, durability, and storage, are essential factors in streamlining the regulatory approval process and improving the manufacturability of liposomal drug delivery systems. Furthermore, regardless of charge, the released Lip elevated the pro-inflammatory cytokines, thereby enhancing osteogenesis and thus being ideal for orthopedic applications. In the future, this liposomal coating technology can be used as a platform for the local delivery of any Lip with or without cargo in biomedical and clinical applications.

CRediT authorship contribution statement

F. Jahanmard: Conceptualization, Methodology, Validation, Formal analysis, Investigation, Visualization, Project administration, Writing – original draft. **A. Khodaei:** Formal analysis, Investigation, Writing – review & editing. **J. Flapper:** Formal analysis, Investigation, Writing – review & editing. **O. Dogan:** Formal analysis, Investigation, Writing – review & editing. **K. Roohi:** Formal analysis, Investigation, Writing – review & editing. **P. Taheri:** Resources, Supervision, Writing – review & editing. **H. Weinans:** Resources, Writing – review & editing. **G. Storm:** Writing – review & editing. **M. Croes:** Conceptualization, Funding

acquisition, Writing – review & editing. **E. Mastrobattista:** Funding acquisition, Project administration, Supervision, Writing – review & editing. **S. Amin Yavari:** Conceptualization, Resources, Project administration, Supervision, Writing – review & editing.

Data availability

Data will be made available on request.

Acknowledgment

The research for this paper was financially supported by the Phospholipid Research Center funding program.

References

[1] D. Holmes, Non-union bone fracture: a quicker fix, Nature 550 (7677) (2017) S193.
[2] L.A. Mills, S.A. Aitken, A.H.R. Simpson, The risk of non-union per fracture: current myths and revised figures from a population of over 4 million adults, Acta Orthop. 88 (4) (2017) 434–439.
[3] G. Zhu, et al., Bone physiological microenvironment and healing mechanism: basis for future bone-tissue engineering scaffolds, Bioact. Mater. 6 (11) (2021) 4110–4140.
[4] W. Zhang, et al., Periosteum and development of the tissue-engineered periosteum for guided bone regeneration, J. Orthopaed. Transl. 33 (2022) 41–54.
[5] H. Wei, et al., Recent advances in smart stimuli-responsive biomaterials for bone therapeutics and regeneration, Bone Res. 10 (1) (2022) 1–19.
[6] C.R. Simpson, H.M. Kelly, C.M. Murphy, Synergistic use of biomaterials and licensed therapeutics to manipulate bone remodelling and promote non-union fracture repair, Adv. Drug Deliv. Rev. 160 (2020) 212–233.
[7] A.R. Armiento, et al., Functional biomaterials for bone regeneration: a lesson in complex biology, Adv. Funct. Mater. 30 (44) (2020) 1909874.
[8] F. Jahanmard, et al., Bactericidal coating to prevent early and delayed implant-related infections, J. Control. Release 326 (2020) 38–52.
[9] B. Akhavan, et al., Radical-functionalized plasma polymers: stable biomimetic interfaces for bone implant applications, Appl. Mater. Today 16 (2019) 456–473.
[10] S. Bohara, J. Suthakorn, Surface coating of orthopedic implant to enhance the osseointegration and reduction of bacterial colonization: a review, Biomater. Res. 26 (1) (2022) 26.
[11] B. Zhang, et al., Toward a better regeneration through implant-mediated immunomodulation: harnessing the immune responses, Adv. Sci. 8 (16) (2021) 2100446.
[12] K. Schmidt-Bleek, et al., Boon and bane of inflammation in bone tissue regeneration and its link with angiogenesis, Tissue Eng. B Rev. 21 (4) (2015) 354–364.
[13] S.-K. Lee, J. Lorenzo, Cytokines regulating osteoclast formation and function, Curr. Opin. Rheumatol. 18 (4) (2006) 411–418.
[14] T. Zhang, Y. Yao, Effects of inflammatory cytokines on bone/cartilage repair, J. Cell. Biochem. 120 (5) (2019) 6841–6850.
[15] W. Wang, K.W. Yeung, Bone grafts and biomaterials substitutes for bone defect repair: a review, Bioactive Mater. 2 (4) (2017) 224–247.
[16] T.A. Einhorn, L.C. Gerstenfeld, Fracture healing: mechanisms and interventions, Nat. Rev. Rheumatol. 11 (1) (2015) 45–54.
[17] H. Newman, Y.V. Shih, S. Varghese, Resolution of inflammation in bone regeneration: from understandings to therapeutic applications, Biomaterials 277 (2021), 121114.
[18] M. Croes, et al., Local induction of inflammation affects bone formation, Eur. Cells Mater. 33 (2017) 211–226.
[19] E. Zhang, et al., Role of TNF-α in early-stage fracture healing under normal and diabetic conditions, Comput. Methods Prog. Biomed. 213 (2022), 106536.
[20] J. Deng, et al., Tailoring the physicochemical properties of nanomaterials for immunomodulation, Adv. Drug Deliv. Rev. 180 (2022), 114039.
[21] S. Antimisiaris, et al., Overcoming barriers by local drug delivery with liposomes, Adv. Drug Deliv. Rev. 174 (2021) 53–86.
[22] B. Sheikholeslami, et al., Exploring the impact of physicochemical properties of liposomal formulations on their in vivo fate, Life Sci. 300 (2022), 120574.
[23] X. Lai, et al., Light-triggered efficient sequential drug delivery of biomimetic Nanosystem for multimodal chemo-, antiangiogenic, and anti-MDSC therapy in melanoma, Adv. Mater. (2022) 2106682.
[24] Y. Liu, et al., Photoresponsive vaccine-like CAR-M system with high-efficiency central immune regulation for inflammation-related depression, Adv. Mater. 34 (11) (2022) 2108525.
[25] Q. Shang, et al., Local scaffold-assisted delivery of immunotherapeutic agents for improved cancer immunotherapy, Adv. Drug Deliv. Rev. 185 (2022) 114308.
[26] N. Monteiro, et al., Antibacterial activity of chitosan nanofiber meshes with liposomes immobilized releasing gentamicin, Acta Biomater. 18 (2015) 196–205.
[27] V. De Leo, et al., Liposome-modified titanium surface: a strategy to locally deliver bioactive molecules, Colloids Surf. B: Biointerfaces 158 (2017) 387–396.
[28] E. Pugliese, J.Q. Coentro, D.I. Zeugolis, Advancements and challenges in multidomain multicargo delivery vehicles, Adv. Mater. 30 (13) (2018) 1704324.
[29] C. Tan, J. Wang, B. Sun, Biopolymer-liposome hybrid systems for controlled delivery of bioactive compounds: recent advances, Biotechnol. Adv. 48 (2021), 107727.
[30] J.Y. Yu, et al., Post-processing techniques for the improvement of liposome stability, Pharmaceutics 13 (7) (2021) 1023.
[31] R. Cheng, et al., Advanced liposome-loaded scaffolds for therapeutic and tissue engineering applications, Biomaterials 232 (2020), 119706.
[32] R. Cheng, et al., Mechanically enhanced lipo-hydrogel with controlled release of multi-type drugs for bone regeneration, Appl. Mater. Today 12 (2018) 294–308.
[33] H.S. O'Neill, et al., A stimuli responsive liposome loaded hydrogel provides flexible on-demand release of therapeutic agents, Acta Biomater. 48 (2017) 110–119.
[34] W. Li, et al., Tough bonding, on-demand debonding, and facile rebonding between hydrogels and diverse metal surfaces, Adv. Mater. 31 (48) (2019) 1904732.
[35] Y.N. Ye, et al., Tough and self-recoverable thin hydrogel membranes for biological applications, Adv. Funct. Mater. 28 (31) (2018) 1801489.
[36] N. Bentley, et al., Protein repellent, surface-attached hydrogels through spray coating, Adv. Mater. Interfaces (2022) 2102359.
[37] L. Abi Nassif, et al., Electrophoretic deposition of zinc alginate coatings on stainless steel for marine antifouling applications, J. Environ. Chem. Eng. 8 (5) (2020), 104246.
[38] S.K. Boda, X. Li, J. Xie, Electrospraying an enabling technology for pharmaceutical and biomedical applications: a review, J. Aerosol Sci. 125 (2018) 164–181.
[39] G. Rouser, S. Fleischer, A. Yamamoto, Two dimensional thin layer chromatographic separation of polar lipids and determination of phospholipids by phosphorus analysis of spots, Lipids 5 (5) (1970) 494–496.
[40] F.P. Melchels, et al., Development and characterisation of a new bioink for additive tissue manufacturing, J. Mater. Chem. B 2 (16) (2014) 2282–2289.
[41] Q. Yu, et al., Thickness measurement for glass slides based on chromatic confocal microscopy with inclined illumination, in: Photonics, Multidisciplinary Digital Publishing Institute, 2021.
[42] M. Croes, et al., Inflammation-induced osteogenesis in a rabbit tibia model, Tissue Eng. Part C: Methods 23 (11) (2017) 673–685.
[43] I. Pennings, et al., Effect of donor variation on osteogenesis and vasculogenesis in hydrogel cocultures, J. Tissue Eng. Regen. Med. 13 (3) (2019) 433–445.
[44] P.M. Mountziaris, A.G. Mikos, Modulation of the inflammatory response for enhanced bone tissue regeneration, Tissue Eng. B Rev. 14 (2) (2008) 179–186.
[45] T. Liu, et al., Effect of freezing process on the microstructure of gelatin Methacryloyl hydrogels, Front. Bioeng. Biotechnol. (2021) 1306.
[46] M. Maruyama, et al., Modulation of the inflammatory response and bone healing, Front. Endocrinol. 11 (2020) 386.
[47] A. Cheng, et al., Early systemic immune biomarkers predict bone regeneration after trauma, Proc. Natl. Acad. Sci. 118 (8) (2021).
[48] C. He, et al., Effects of particle size and surface charge on cellular uptake and biodistribution of polymeric nanoparticles, Biomaterials 31 (13) (2010) 3657–3666.
[49] M.V. Baranov, et al., Modulation of immune responses by particle size and shape, Front. Immunol. (2021) 3854.
[50] P. Foroozandeh, A.A. Aziz, Insight into cellular uptake and intracellular trafficking of nanoparticles, Nanoscale Res. Lett. 13 (1) (2018) 1–12.
[51] H. Yue, et al., Particle size affects the cellular response in macrophages, Eur. J. Pharm. Sci. 41 (5) (2010) 650–657.
[52] F. Zahednezhad, et al., Liposome and immune system interplay: challenges and potentials, J. Control. Release 305 (2019) 194–209.
[53] F. Giulimondi, et al., Interplay of protein corona and immune cells controls blood residency of liposomes, Nat. Commun. 10 (1) (2019) 1–11.
[54] I. Hafez, N. Maurer, P. Cullis, On the mechanism whereby cationic lipids promote intracellular delivery of polynucleic acids, Gene Ther. 8 (15) (2001) 1188–1196.
[55] A.J. Teunissen, et al., Embracing nanomaterials' interactions with the innate immune system, Wiley Interdiscipl. Rev.: Nanomed. Nanobiotechnol. 13 (6) (2021), e1719.
[56] N. Marasini, et al., Liposomes as a vaccine delivery system, in: Micro and Nanotechnology in Vaccine Development, Elsevier, 2017, pp. 221–239.
[57] P. Vermette, et al., Characterization of surface-immobilized layers of intact liposomes, Biomacromolecules 5 (4) (2004) 1496–1502.
[58] S. Cascone, G. Lamberti, Hydrogel-based commercial products for biomedical applications: a review, Int. J. Pharm. 573 (2020), 118803.
[59] S. Zhu, et al., A bottom-up evaluation on cryoprotective potentials of gelatine from fish scale, Food Hydrocoll. 124 (2022), 107243.
[60] P. Guan, et al., Solidification of liposomes by freeze-drying: the importance of incorporating gelatin as interior support on enhanced physical stability, Int. J. Pharm. 478 (2) (2015) 655–664.
[61] J. Cao, et al., Dual physical crosslinking strategy to construct moldable hydrogels with ultrahigh strength and toughness, Adv. Funct. Mater. 28 (23) (2018) 1800739.
[62] H. Zhang, et al., Multifunctional crosslinking-enabled strain-regulating crystallization for stable, efficient α-FAPbI3-based perovskite solar cells, Adv. Mater. 33 (29) (2021) 2008487.
[63] W. Zhang, et al., Promoting Oral mucosal wound healing with a hydrogel adhesive based on a Phototriggered S-Nitrosylation coupling reaction, Adv. Mater. 33 (48) (2021) 2105667.
[64] H. Ravanbakhsh, et al., Emerging Technologies in Multi-Material Bioprinting, Adv. Mater. 33 (49) (2021) 2104730.
[65] Y. Hou, X. Deng, C. Xie, Biomaterial surface modification for underwater adhesion, Smart Mater. Med. 1 (2020) 77–91.
[66] J. Liu, et al., Functional hydrogel coatings, Natl. Sci. Rev. 8 (2) (2021) nwaa254.

[67] Y. Wang, et al., Instant, tough, noncovalent adhesion, ACS Appl. Mater. Interfaces 11 (43) (2019) 40749–40757.
[68] C. Wu, et al., All electrospray printing of carbon-based cost-effective perovskite solar cells, Adv. Funct. Mater. 31 (6) (2021) 2006803.
[69] T.C. Nguyen, W.-S. Choi, Electrospray mechanism for quantum dot thin-film formation using an electrohydrodynamic jet and light-emitting device application, Sci. Rep. 10 (1) (2020) 1–9.
[70] Z. Zhong, et al., Membrane surface roughness characterization and its influence on ultrafine particle adhesion, Sep. Purif. Technol. 90 (2012) 140–146.
[71] J. Pajarinen, et al., Mesenchymal stem cell-macrophage crosstalk and bone healing, Biomaterials 196 (2019) 80–89.
[72] S.B. Goodman, M. Maruyama, Inflammation, bone healing and osteonecrosis: from bedside to bench, J. Inflamm. Res. 13 (2020) 913.
[73] C. Hoemann, H. El-Gabalawy, M. McKee, In vitro osteogenesis assays: influence of the primary cell source on alkaline phosphatase activity and mineralization, Pathol. Biol. 57 (4) (2009) 318–323.
[74] M. Croes, et al., Proinflammatory mediators enhance the osteogenesis of human mesenchymal stem cells after lineage commitment, PLoS One 10 (7) (2015), e0132781.
[75] J.K. Chan, et al., Low-dose TNF augments fracture healing in normal and osteoporotic bone by up-regulating the innate immune response, EMBO Mol. Med. 7 (5) (2015) 547–561.
[76] A.P. Bastidas-Coral, et al., Cytokines TNF-α, IL-6, IL-17F, and IL-4 differentially affect osteogenic differentiation of human adipose stem cells, Stem Cells Int. 2016 (2016).
[77] W.M. Groen, et al., Impact of endotoxins in gelatine hydrogels on chondrogenic differentiation and inflammatory cytokine secretion in vitro, Int. J. Mol. Sci. 21 (22) (2020) 8571.